Proceedings of the ASME 2010 3rd Joint US-European Fluids Engineering Summer Meeting and 8th International Conference on Nanochannels, Microchannels, and Minichannels
FEDSM-ICNMM2010
August 1-5, 2010, Montreal, Canada

FEDSM-ICNMM2010-30824

EMBEDDED REFRACTIVE INDEX SENSING IN MICROCHANNELS USING MULTIPLEXED SILICON-ON-INSULATOR MICRORING RESONATORS

Michael Grad
Columbia University
New York, NY, USA

Daniel Attinger
Columbia University
New York, NY, USA

Chee Wei Wong
Columbia University
New York, NY, USA

ABSTRACT

We describe the use of wavelength-multiplexed microring resonators as refractive index sensors embedded in microfluidic channels for parallel and differential sensing. The sensor geometry consists of two or more identical 45-micron diameter silicon ring resonators fabricated on silicon dioxide coupled to a single input/output bus waveguide. Two modes of sensing are described: parallel sensing with multiple sensors embedded in separate fluidic channels, and increased sensitivity refractive index sensing by the compensation of temperature dependence with a differential temperature referencing measurement. The first set of experiments demonstrates parallel sensing of water and aqueous salt solutions embedded in separate microchannels. The second set of experiments demonstrates the removal of temperature dependence, and thus improved refractive index detection limit, by temperature referencing using a differential measurement between two resonators.

1. INTRODUCTION

The miniaturization of chemical reactions involved with Lab-on-a-chip is driven by decreased sample volumes and reaction times at small scales, however these come at a loss of throughput associated with smaller systems. The solution has been to perform these chemical reactions in parallel microfluidic channels to maintain the faster reaction times and high throughputs. The ability to sense what is happening in these parallel microchannels, therefore, is important to Lab-on-a-chip.

An important feature of optofluidic technologies is the ability to perform refractive index sensing using optical cavities, which can detect a variety of changes in the fluid such as concentration, temperature, chemistry and physical phases [1-7]. It has been demonstrated that resonant wavelength of optical cavities is sensitive to slight changes in these parameters in bulk solution [1, 7] and in microfluidic channels [2, 3]. Also, these resonators have been used for time-resolved sensing of liquid films in microfluidic channels [3]. Further, two resonators can be coupled to a single bus waveguide, and the ir resonant peaks can be tracked separately. This multiplexed configuration has been used with polymer waveguides to sense both the temperature and concentration of a bulk solution [8], and with slot waveguide resonator arrays and photonic crystal resonator arrays embedded in microfluidic channels [5, 9] as refractive index and biosensors. This paper shows two modes of sensing with multiple resonators coupled to a single bus waveguide: (1) parallel sensing with the resonators embedded in separate parallel microchannels, and (2) temperature-compensated refractive index sensing using a differential measurement between a sensing microchannel and a reference microchannel.

Parallel sensing is important to Lab-on-a-Chip. Because the resonant sensors described in this paper can have different resonant wavelengths, they can be used as multiplexed parallel sensors coupled to a single bus waveguide. This allows the sensing in several parallel microchannels, with no more light sources or output detectors than required in a single sensor scheme. This sensing mode will be discussed in section 3.

A sensor's refractive index detection limit (DL) is defined as the ratio of the resolution R (determined by the noise of the system), and the sensitivity of the resonator to refractive index changes, (S ~ $d\lambda/dn$), where DL=R/S [3, 6]. Current detection limits reach values of 10^{-5}-10^{-7} refractive index units (RIU) [1-7]. Noise, and specifically thermal noise induced by temperature fluctuations, is a major factor in the detection limit of the individual resonant sensors cited above [6]. Currently one noise-reduction method is temperature stabilization [6]. Here, we propose to compensate for the temperature dependence by implementing a differential sensing scheme. This scheme will be discussed in section 4.

2. SENSOR CONFIGURATIONS AND GEOMETRY

The two modes of sensing described in sections 3 and 4, i.e. parallel and differential sensing, are both implemented on the same geometry: two or more ring resonators coupled in series to a single bus waveguide. Figure 1 shows a picture of the rings, and a schematic of the rings embedded in microfluidic channels.

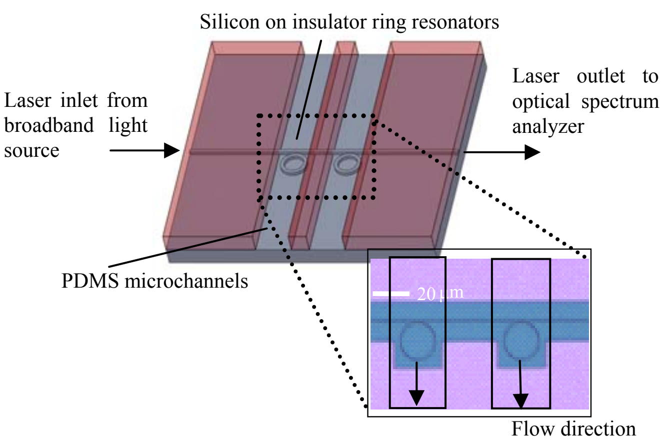

Figure 1: geometry of resonator chip and integrated microfluidic channels. Light is coupled to the waveguide from optical fibers with a ~2μm Gaussian waist, and the PDMS microchannels are aligned over the resonators perpendicular to the waveguides.

The input light to the waveguide is fed along a tapered optical fiber with a ~2μm Gaussian waist from a broadband source (amplified spontaneous emission, or ASE) with wavelengths between 1500nm to 1580nm. The output from the waveguide is fed along a similar fiber into an optical spectrum analyzer, or OSA, capable of scanning the 80nm range in under 10 seconds with resolution of 0.05 nm. Figure 2 shows a narrow bandwidth sample output from the OSA, where transmission intensity is plotted against the wavelength. In the black curve, two resonant valleys appear in the same spectrum, corresponding to the contribution of the two ring resonators. This figure will be analyzed further in the next section.

The high refractive index contrast between silicon and the silicon dioxide substrate confines the light in the waveguides due to total internal reflection. At the surface of the waveguides, some light escapes approximately 400nm into the surrounding environment [3], producing an evanescent field in the surrounding fluid. Perturbations to this evanescent field cause shifts to the resonant wavelength of the ring resonators. In our setup, microfluidic channels are used to bring samples within sensing distance of the ring resonators. By placing separate channels over each resonator, we can target each sensor with a different fluid sample to achieve either parallel sensing or temperature referenced sensing, as will be discussed in the following sections.

3. MODE I: MULTIPLEXED (OR PARALLEL) SENSING

Using the geometry described above, the first sensing mode uses each ring as a separate sensor. Since both rings are coupled to the same bus waveguide, this parallel sensing configuration increases the number of sensors without increasing the number of laser inputs and detectors. Barring any cross-talk between resonators by embedding them into separate microfluidic channels, refractive index changes of the fluid in each channel will only cause resonant shifts to their respective resonator. This is tested below by flowing different fluids through each channel and measuring the intensity spectrum of the light at the output waveguide.

Experimental results

Using the geometry described in section 2 and the multiplexed sensing mode described above, figure 2 shows experimental results from two testing conditions. For the blue curve, both microfluidic channels were filled with water, and the resonant peaks (shown by the blue circles) overlap at a single resonant wavelength (~1572.7 nm). For the black curve, the first microfluidic channel remained filled with water, and the second microfluidic channel was filled with a 3% aqueous salt solution. The first resonant peak remained at the same wavelength, but the second resonant peak shifted because of the refractive index perturbation caused by the salt solution. Therefore the black curve shows two resonant peaks separated by almost 0.5nm. While figure 2 shows the parallel sensing capabilities with only two resonators, this approach can be extrapolated to three or more resonators coupled to the same bus waveguide. Also, the rings shown in figure two are identical and therefore overlap for the same fluid. The disadvantage with this situation is that the first resonant peak can mask very small perturbations to the second resonance. To solve this issue, it is possible to use two rings with different diameter or gap spacing, thus tuning their resonant wavelength to be different. In this configuration, each resonant peak can be track completely separately, and the second peak will not hide small changes to resonant wavelength.

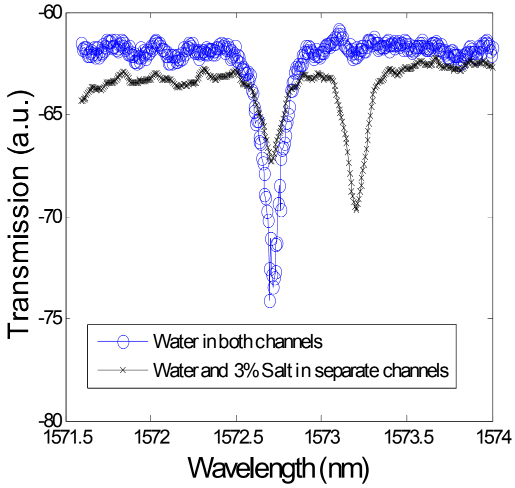

Figure 2: multiplexed sensing of water and 3% salt. When water fills both channels (blue curve), the two resonances overlap. When water is in the first channel and an aqueous salt solution fills the second channel (black curve) there are two resonant peaks corresponding to the different indices of refraction.

4. MODE II: DIFFERENTIAL MEASUREMENTS FOR TEMPERATURE REFERENCING

The sensor's refractive index detection limit (DL) is defined as the ratio of the resolution R (determined by the noise of the system), and the sensitivity of the resonator to refractive index changes, (S ~ $d\lambda/dn$), where DL=R/S [3, 6]. Therefore a major limitation to the detection limit of the single resonator sensors discussed in section 1 is the noise of the system, specifically thermal noise introduced by temperature fluctuations caused by the laser or by environmental factors [6]. We propose to eliminate the thermal noise by implementing a differential sensing to reference out the noise. In this scheme, using the geometry described in section two, the two channels will be designated as a sensing channel and a reference channel. The reference channel will always be filled with water, while the sensing channel will be exposed to different indexed fluids. Instead of tracking the absolute value of the resonant wavelength of the sensing channel, we propose to track the difference between the reference channel and the sensing channel. Temperature fluctuations from the environment or laser should cause both peaks to shift together, maintaining the same differential value but a different absolute value of resonant wavelength.

Experimental results

Using the geometry described in section 2 and the sensing configuration described above, an experiment was performed to measure the values of resonant wavelength at different temperatures. A 100W cartridge heater (Omega, USA) embedded in the brass mounting platform was operated without feedback control at constant DC voltage and the system was left to reach steady state. The temperature was measured just beneath the sensing chip by a thermocouple (K Type, Omega). The channels were filled with water and 3% aqueous salt solution.

Figure 3 shows the temperature-induced drift from the differential and absolute sensing modes. Figure 3a shows the output from the sensors from two tests where the temperature was altered by 15 degrees. For the first test at 33 degrees (shown in red), two resonant peaks are noticeable corresponding to the two resonators coupled to the bus waveguide. At the higher temperature (shown in black), it can be seen that these two peaks shifted simultaneously towards the red end of the spectrum. An absolute wavelength shift of approximately 1.5 nm is induced by the change to temperature, while the relative distance between resonant peaks and the shape of the resonances is not noticeably affected. Figure 3b shows these same shifts as a function of temperature for the absolute (i.e. only track λ_1) and differential modes of sensing (i.e. track the difference between λ_1 and λ_2). From figure 3b, it can be seen that differential sensing removes the dependence of the ring resonators on temperature. Future work for this project includes the direct comparison of detection limits in the differential sensing configuration compared to a single sensor.

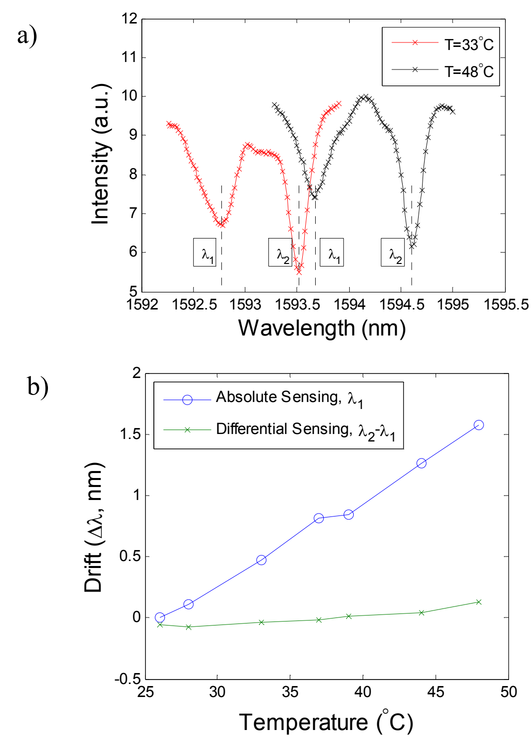

Figure 3: Temperature-induced drift of resonant wavelength: a) transmission intensity as a function of wavelength showing the two resonant peaks at two different temperatures. b) the quantification of figure a for a series of temperatures between 26 and 48 degrees. The blue curve represents the value of the first resonant wavelength, λ_1, as a function of temperature, normalized to 26 degrees. The green curve represents the difference between resonant peaks, λ_2-λ_1, as a function of temperature.

5. CONCLUSION

We have demonstrated the ability to use wavelength-multiplexed silicon on insulator ring resonators as parallel and differential sensors embedded in microfluidic channels. The first set of experiments demonstrated parallel sensing of aqueous salt solutions using two ring resonators, and the extrapolation to more sensors was discussed. The second set of experiments demonstrated the ability to remove the temperature-induced drift of a sensor with in-situ referencing to a second resonator using a differential measurement. The implications of this work are improved detection limit of refractive index sensing using these resonators by decreasing thermal noise. Future work includes direct comparison of detection limit with previously published sensors.

6. ACKNOWLEDGEMENTS

The authors would like to acknowledge funding support from NSF grant 0701729 and the Mechanical Engineering department at Columbia University.

7. REFERENCES

1. Chao, C.Y., W. Fung, and L.J. Guo, *Polymer microring resonators for biochemical sensing applications.* IEEE Journal on Selected Topics in Quantum Electronics, 2006. **12**(1): p. 134-142.
2. De Vos, K., I. Bartolozzi, E. Schacht, P. Bienstman, and R. Baets, *Silicon-on-Insulator microring resonator for sensitive and label-free biosensing.* Optics Express, 2007. **15**(12): p. 7610-7615.
3. Grad, M., C.C. Tsai, M. Yu, D.-L. Kwong, C.W. Wong, and D. Attinger, *Transient sensing of liquid films using optofluidic microresonators.* Measurement Science and Technology, submitted 2010.
4. Ksendzov, A. and Y. Lin, *Integrated optics ring-resonator sensors for protein detection.* Optics Letters, 2005. **30**(24): p. 3344-3346.
5. Mandal, S. and D. Erickson, *Nanoscale optofluidic sensor arrays.* Optics Express, 2008. **16**(3): p. 1623-1631.
6. White, I.M. and X. Fan, *On the performance quantification of resonant refractive index sensors.* Optics Express, 2008. **16**(2): p. 1020-1028.
7. Yalçin, A., K.C. Popat, J.C. Aldridge, T.A. Desai, J. Hryniewicz, N. Chbouki, B.E. Little, O. King, V. Van, S. Chu, D. Gill, M. Anthes-Washburn, M.S. Ünlü, and B.B. Goldberg, *Optical sensing of biomolecules using microring resonators.* IEEE Journal on Selected Topics in Quantum Electronics, 2006. **12**(1): p. 148-154.
8. Kwon, M.S. and W.H. Steier, *Microring-resonator-based sensor measuring both the concentration and temperature of a solution.* Optics Express, 2008. **16**(13): p. 9372-9377.
9. Carlborg, C.F., K.B. Gylfason, A. Kamierczak, F. Dortu, M.J. Bauls Polo, A. Maquieira Catala, G.M. Kresbach, H. Sohlstram, T. Moh, L. Vivien, J. Popplewell, G. Ronan, C.A. Barrios, G. Stemme, and W. Van Der Wijngaart, *A packaged optical slot-waveguide ring resonator sensor array for multiplex label-free assays in labs-on-chips.* Lab on a Chip - Miniaturisation for Chemistry and Biology. **10**(3): p. 281-290.

